SSIM 2025 - JJ Potter & J Wesseloo (eds)

doi:10.36487/ACG_repo/2535_37

An update to kinematic analysis of pit shells

Samson Tims [a,*], **Julian Venter** [b]

[a] *SRK Consulting, Canada*

[b] *AngloGold Ashanti, Australia*

Abstract

The original methodology presented by Venter et al. (2018) and Venter & Hamman (2022) for simplified probabilistic kinematic analyses applied on pit shells, has been updated and modified based on usage for design and performance reconciliation. The underlying logic of assessing kinematic risks for pit shells remains unchanged by assessing probability of occurrence for the main kinematic failure types of planar and wedge, sliding and flexural, and direct toppling. This paper will present some practical use cases of the tool beyond which were originally envisioned, including validation of design joint sets for reconciliation purposes. In addition, the paper will present an additional workflow that allows for discretely assessing the likelihood of forming double plane failures against modelled faults, which can be used to assess risks for ramp placement for example.

Keywords: *kinematic analysis, slope stability, automation*

1 Introduction

Kinematic analyses are used to understand the potential risks for structurally controlled failures in hard rocks. The simplified kinematic analysis proposed by Venter & Hamman (2022), using geometric constraints for sliding and toppling failure types (Goodman 1980; Hudson & Harrison 2000), has proven to be an effective tool in understanding spatial risks related to kinematic failures. These calculations are largely based on stereonet kinematic analyses but address some of the limitations to unfiltered assessments using potentially biased or under-sampled data by using the characteristics of identified joint sets. The ability to colourise pit shells by the probability of occurrence for each main failure mode as a potential risk map, serves as an effective communication tool for stakeholders that may not be geotechnical engineers. Experience in using the Venter & Hamman (2022) tool has shown that the probabilistic estimates obtained can be conservative, as not all the essential conditions needed for kinematic failures have been addressed in the original paper and its supporting papers. There is a myriad of literature available discussing geometric constraints on block formation and application of kinematic analyses that will not be directly discussed in this paper, but were used to inform these calculations (Hoek & Bray 1981; Goodman & Shi 1985; Wyllie & Mah 2004).

This paper serves as an update to the initial methodology for calculating probability of occurrence based on usage for a range of structurally controlled deposits. Modifications to the calculations have come as a result of being unable to visualise certain known failure modes based on the contributing joint sets, as well as a desire for better integration of structural models into the kinematic assessment. As such, this paper modifies the requirements for planar failure by adding a requirement for a minimum persistence, to enable back-break to be used as design acceptance. The flexural and direct toppling failure modes are also modified to include the need for block aspect ratios. These additions are made by first presenting some lessons learned in the application of the methodology, followed by the additions to the original methodology.

* Corresponding author. Email address: stims@srk.com

2 Lessons learned

The use of the simplified kinematic analysis has expanded beyond the initial intention of evaluating design shells against a geotechnical block model. This tool has found significant use in early-stage assessments of kinematic risks before using more advanced probabilistic or numerical modelling tools. The authors have developed additional outputs and tools using Python to inform geotechnical analyses of open pits as a consultant. Programming, compared to using a spreadsheet, to develop the code takes advantage of numerous pre-built packages for managing data as well as enabling the ability to iterate and loop through various combinations of discontinuities. Using the tool on operating mines has allowed for a careful consideration of the required outputs from the tool, as well as modifications to the calculations required to better reflect reality. Some of the most useful applications of the automated kinematics are presented below.

2.1 Summary of results

One of the frustrations of completing kinematic analyses on multiple joint sets is understanding which sets are contributing to particular failure modes without tediously and manually following the planes and intersections across a stereonet for the full range of slope azimuths. The authors developed code to compute the kinematics on any increment of slope azimuths and output the results.

The authors have found the automatic generation of tables of contributing joint sets useful for assessment and reporting. The probability of occurrence is binned into categories: low (<25%), moderate (25–50%) and high (>50%). One of the outputs that can be programmed will output all sets or combinations of sets with a probability of occurrence greater than a certain threshold, with >10% likelihood proving a reasonable starting point for assessment (Table 1). This both simplifies reporting requirements as well as highlights specific joint combinations to assess in further detail, using Rocscience's SWedge for example.

Table 1 Example table output highlighting contributing discontinuities per failure mode for the full range of slope azimuths

Slope dip direction (°)	Mode of instability					
	Planar sliding		Wedge sliding		Direct topple	
	Probability	Sets	Probability	Sets	Probability	Sets
0	High	JS1			High	JS2-JS6, JS3-JS5
20	High	JS1			High	JS2-JS6, JS3-JS5
40	High	JS1			High	JS2-JS6, JS3-JS5
60	Low	JS1			Moderate	JS3-JS4
80			Low	JS1-JS5	High	JS3-JS4
100			Low	JS1-JS5	Low	JS3-JS4
120					Low	JS1-JS2
140	Moderate	JS5			High	JS1-JS2
160	Moderate	JS5			High	JS1-JS2, JS1-JS3
180	Moderate	JS5			High	JS1-JS2, JS1-JS3
200					Moderate	JS1-JS3
220						
240						
260					Low	JS2-JS6
280					Low	JS2-JS6
300					Moderate	JS2-JS3, JS2-JS6
320					High	JS2-JS3, JS2-JS5, JS2-JS6
340	Moderate	JS1			High	JS2-JS3, JS2-JS5, JS2-JS6
360	High	JS1			High	JS2-JS6, JS3-JS5

2.2 Validation of design joint sets

Considering the outputs of the calculations, a colourised pit shell and table of contributing joint sets, a review of the design sets can be undertaken. For any given sector of the open pit, failure modes and contributing features should be identified and compared to the predicted outputs from the automated kinematic assessment (Figure 1). This requires reviewing these sectors and ensuring that:

- the predicted range of affected wall azimuths and the actual wall correlate
- the contributing joint sets match with the visible failures.

Should there be disagreement between the predicted outcome from the automated kinematics and the as-built, the user should revisit the joint sets selected for validity and consider modifications of the inputs as required – to align with the actual performance. This may include revising the inputs for the joint sets or redefining the joint sets for the particular domain. These steps are considered critical to establishing reliable bench designs by understanding the potential risks from dominant structural families.

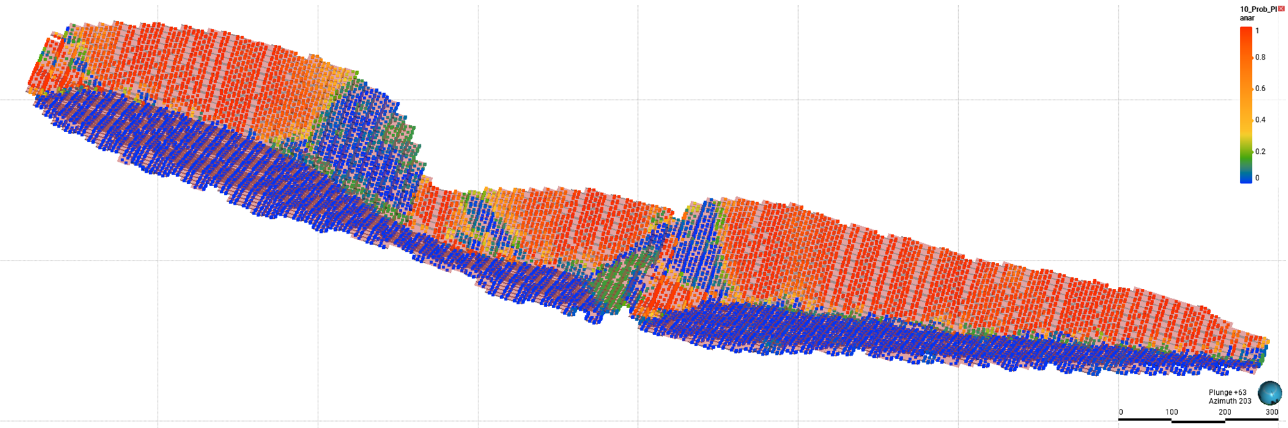

Figure 1 Example output showing probability of occurrence for planar failures. This should be reviewed against the as-built shell for validation of design sets and inputs

2.3 Adapting the workflow for optimisation shells

The initial paper computes against pit design wireframes, with generally reliable adherence to implementation. As a consultant, we are provided with a range of pit designs, from optimisation shells without designed benches nor ramps, to highly detailed photogrammetry surveys. To account for this, the code that the authors developed does not consider the dip of the individual triangles that make up the wireframes and instead uses a user-defined batter angle, generally set to 75°. When presented with high-resolution scan data, localised failures and bench irregularities will show up in the results. In order to use these data, if simplified design shells are not available, the following workflow can be applied to generate a smoothed mesh (Figure 2).

1. load mesh into Gem4D (Basson 2025)
2. subdivide lines/polys to size to regularise the mesh
3. export Polyfaces info as .csv
4. load point cloud into Leapfrog Geo (Seequent 2025) and estimate structural data for point cloud
5. generate a new mesh in Leapfrog using the estimated structural data at a resolution of your choosing. Higher resolutions may show local undulations or changes in azimuth that aren't real, while lower resolutions may show more abrupt changes in probability of occurrence results
6. load mesh into Gem4D and export Polyfaces info as .csv.

Once the kinematics are computed onto the point cloud, these can be loaded back into Gem4D and flagged onto the initial, high-resolution scan point cloud using the 'Value Transfer' function. This enables the results to be draped back onto the initially provided wireframe.

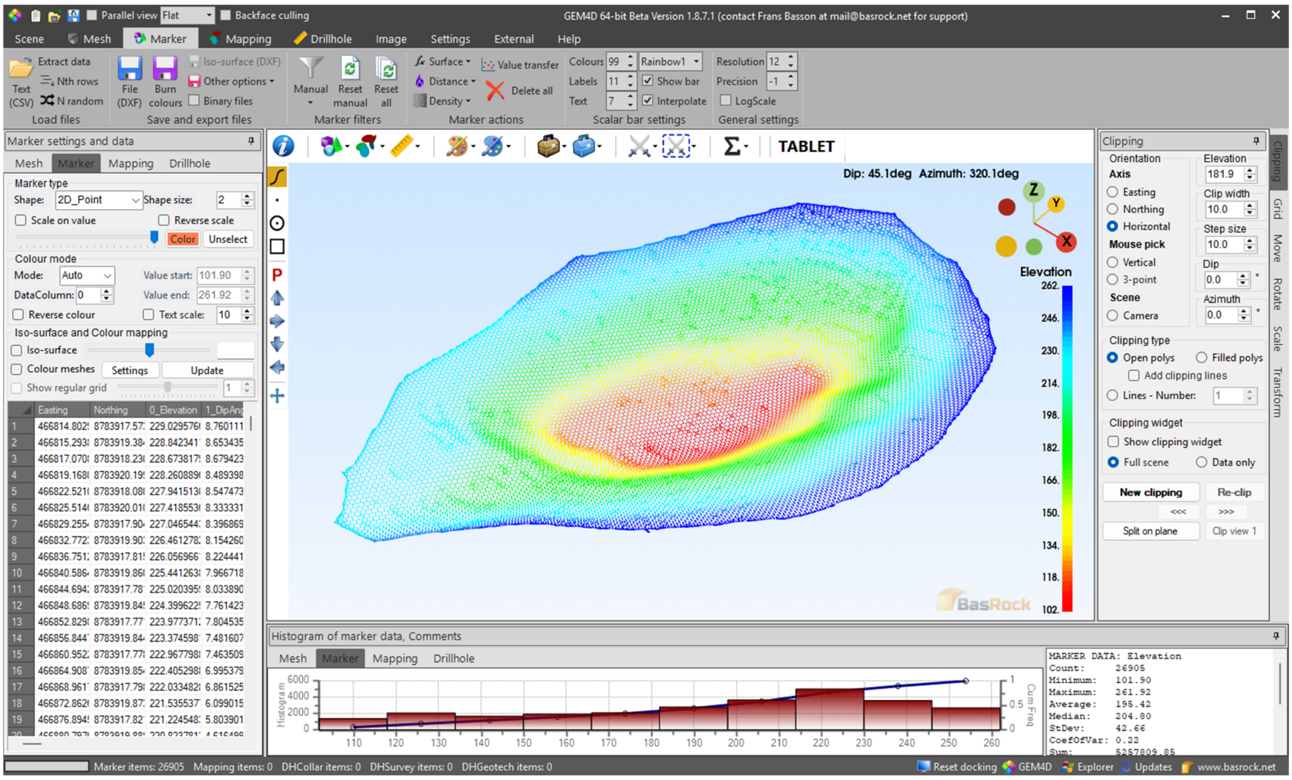

Figure 2 Example of a smoothed pit shell generated from high-resolution scan data

2.4 Fault assessment

Brittle structural models have grown increasingly complex recently with access to improved and faster geological modelling software. Structural geologists are now able to construct highly detailed models containing in some cases hundreds of unique structures. Computing kinematic analyses on 10's of faults is challenging enough, but nearly impossible, or impossibly tedious if the model contains hundreds. There are 2 scales of failures that are possible on faults: bench to multi-bench failures where faults interact with joints and other discontinuities, and multi-bench to slope scale where faults interact with other faults. The potential for large-scale failures should be addressed using numerical modelling and discrete analyses, rather than a simplified approach. However, fault-on-joint kinematics can play an important role in slope performance and especially in understanding localised risks to the ramp (Figure 3). These assessments can be carried out using the simplified kinematic assessment.

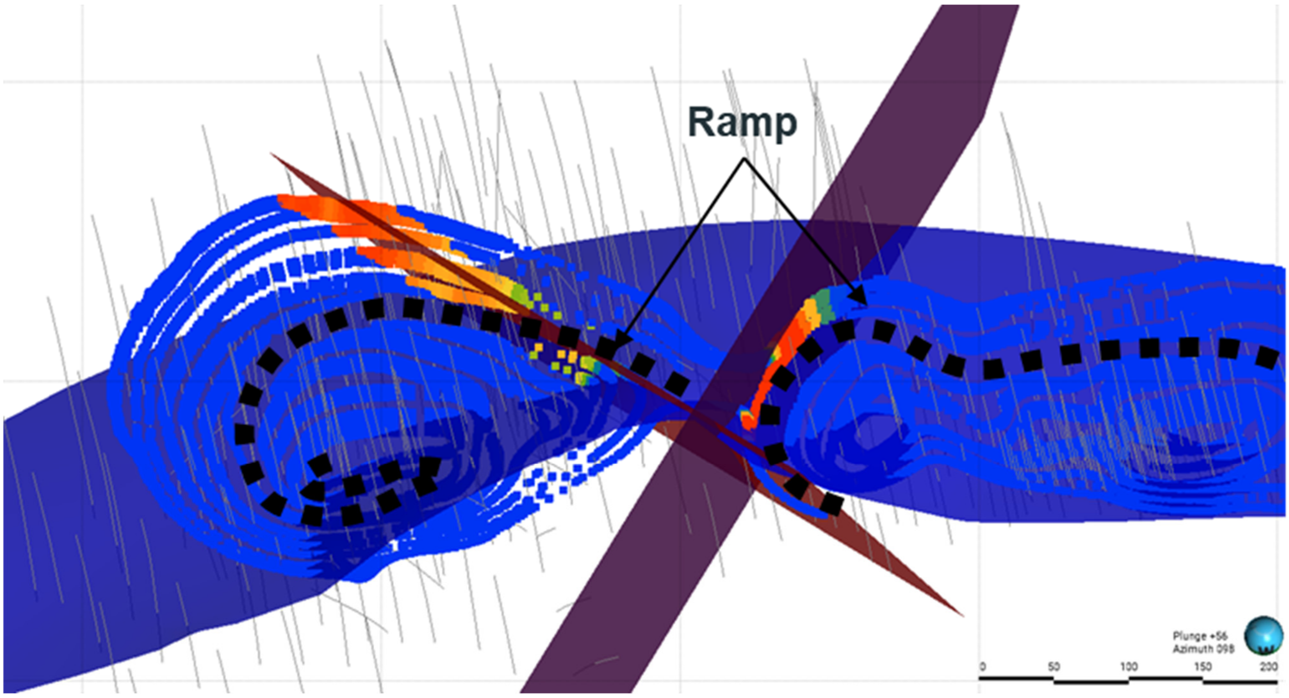

Figure 3 Probability of Occurrence of wedge sliding from joints along the fault planes. The hot colours indicate higher likelihood near the faults, but only for certain slope azimuths

In order to calculate the probability of occurrence for joints-on-fault interactions, the following steps can be undertaken:

1. Calculate the average orientation of each fault plane and assign a representative thickness and shear strength.
2. Compute the distance to each fault surface from the point cloud of the pit shell. This can be used to filter the results to within the fault thickness only.
3. Compute the kinematics for each failure mode for double plane failures (wedge sliding and direct toppling) against the average fault orientation.

The thickness of the fault does not have to be based on the true thickness of the fault but can also account for uncertainty in the position of the fault to flag a particular area of the pit as having potential issues. This tool can be used as a visual representation of potential ramp risks and serve as a discussion point for planning for failure or moving ramp positions.

2.5 The meaning of kinematic probability estimates

Probabilistic kinematic analyses are commonly used to assess the potential risks to a slope dependent on azimuth and bench configuration. These calculations provide an estimated probability of occurrence for each failure type, opposed to a probability of failure for a specific failure. Probability of failure calculations will provide an estimate of the possible range of Factors of Safety (or other suitable performance measure such as displacement) that are possible considering a range of orientations, persistence, and the shear strengths of the contributing planes. Probability of occurrence instead provides an estimate of the likelihood of forming a potentially unstable block within a certain area. As such, these kinematic assessments have proven useful at bench scale level where an open pit comprises several hundred or thousand segments of benches. This methodology is less useful when considering inter-ramp or overall scale slopes where only a few design sectors may be present.

3 Additions to the original methodology

The following sub-sections will detail the geometric constraints for each failure type that are used to inform the probabilistic calculations. The calculations are intended to be relatively simple to implement in either spreadsheets or through basic scripting. Complexity can be added to the calculations if considering more than 3 joint sets, however this becomes challenging to implement within a spreadsheet. Each of these calculations considers a design segment of 10 m length to calculate joint frequency.

3.1 Sliding failures

Planar and wedge sliding failures are the result of sliding of blocks along one or more discontinuities (Figure 4). These failures can be predicted through stereonet analysis by either the relation between the dip of the feature and the orientation of the slope, or the orientation of the intersection line and the orientation of the slope. An oversimplification of the original paper allowed for the probability of intersection within the design segment (Section 3.1.1) for wedges to be considered as the independent probability of intersection of both contributing planes, multiplied by each other. This was problematic as some potentially unstable wedges can form from planes that are potentially stable when considered only for planar sliding failures, yet can generate intersection lines that would otherwise be unstable considering stereonet kinematic analyses.

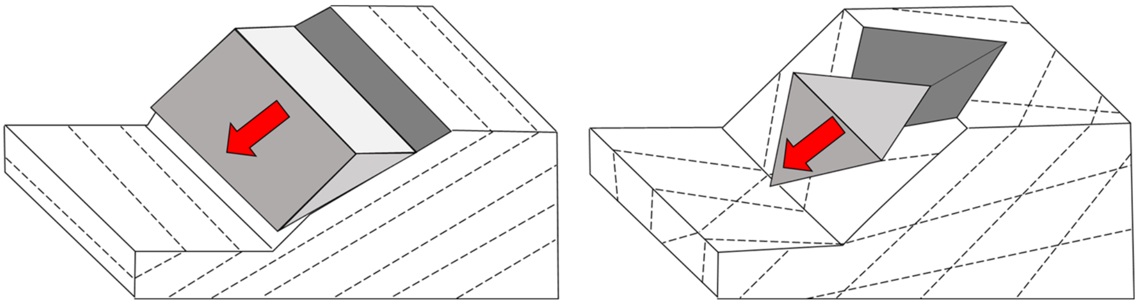

(a) (b)

Figure 4 Planar (a) and wedge (b) sliding failures (after Hudson & Harrison 2000)

Planar and wedge failures can be managed by modifying the bench face angle to reduce the likelihood of instability relative to the dip of the discontinuity or plunge of the intersection line, and by increasing berm widths to manage expected overbreak. Some amount of failure is both expected and non-preventable, and as such the design should attempt to minimise the effects of failures to reduce operator risk and production delays that result from remediating bench and multi-bench scale failures.

Kinematic analysis of planar and wedge sliding considers the probability of occurrence as a function of the following four aspects (Swan & Sepulveda 2001; Venter & Hamman 2022).

3.1.1 Probability of intersection in design segment (C1)

The probability that the persistence of a joint or pair of joints exceeds a minimum length that will cause back-break greater than some acceptable amount (Figure 5). This considers exponential distributions on the spacing, and normal distributions for dip ranges to calculate the minimum persistence length. The minimum persistence required for wedge type failures should be compared against the intersection line and not the individual features as initially proposed. Calculating the minimum persistence required for individual joints has the potential of filtering steep or shallow dipping features that could otherwise contribute to a wedge sliding failure. The original methodology did not consider any limitations to toppling failures, allowing for the possibly formation of blocks that would be fundamentally stable. The modifications to the calculations consider the spacing and persistence of the features, to allow for a more realistic representation of unstable blocks.

Equation 1 provides the estimate for minimum persistence, which needs to be adjusted for features that are steeper than the batter angle that will return an error in the calculation. Equation 2 presents the probability of occurrence within a design segment.

$$Min.Persistence = \frac{Back\text{-}break\ Threshold \times \sin(180° - Batter\ Face\ Angle)}{\sin(Batter\ Face\ Angle - Dip\ or\ Plunge)} \quad (1)$$

$$P[Occurr.in\ Design\ Segment] = 1 - (1 - P[Persistence > \ Min.Persistence])^{Discontinuities\ in\ Segment} \quad (2)$$

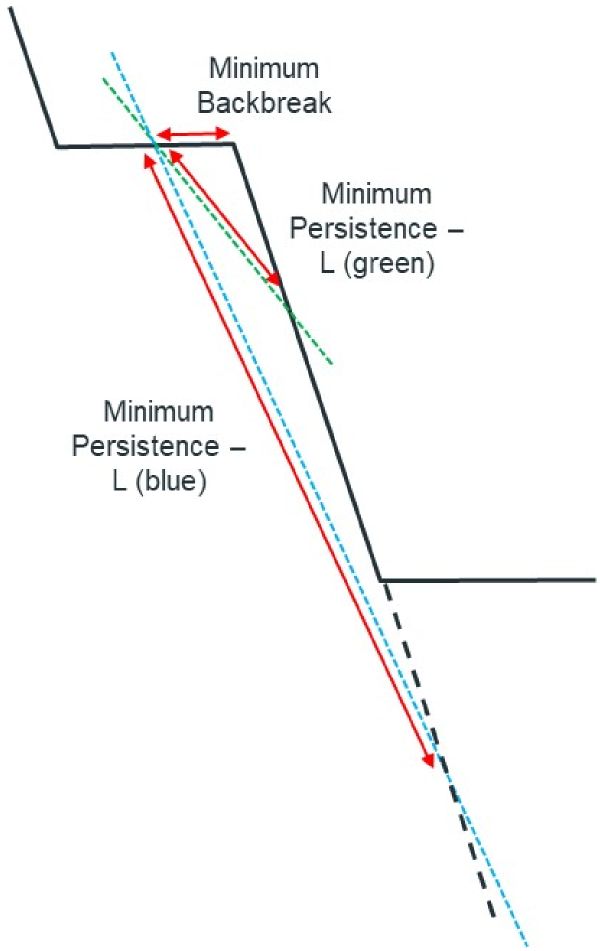

Figure 5 Example of the minimum persistence requirements for a steeply dipping (blue) and moderately dipping feature (green)

3.1.2 Probability of dipping or plunging out of the slope (C2)

The dip direction of the plane or trend of the intersection line must dip out of the slope, a function of the normally distributed range of the discontinuities. The tolerance or acceptable limit can be adjusted depending on preference. For planar sliding failures, possibility of failure is generally considered where the feature dips within 30° of the slope azimuth (Goodman 1980). For wedge sliding failures, the stereonet solution considers any wedge dipping within 90° of the slope as potentially wedge forming. This range may be reduced to 30–45° depending on context.

3.1.3 Probability that dip/plunge > friction angle (C3)

The normally distributed dip or plunge of the feature must be greater than the friction angle for sliding failures to occur. For wedge type failures the minimum friction angle between the 2 surfaces is considered.

3.1.4 Probability that dip/plunge < bench face angle (C4)

The normally distributed dip or plunge of the feature must be less than the bench face angle for the failure to occur.

3.1.5 Probability of occurrence for sliding failures

The probability of occurrence for sliding type failures can be assessed by calculating the probability of achieving each of the geometric constraints, such that the probability of exceeding overbreak can be expressed as Equation 3.

$$P[Sliding\ Failure > Threshold] = C1 \times C2 \times C3 \times C4 \quad (3)$$

where:

C1 = P[batter angle > discontinuity dip or plunge]

C2 = P[ABS(slope azimuth − dip direction (plane) or trend (line) < angular threshold]

C3 = P[discontinuity dip or plunge > friction angle]

C4 = P[occurrence in design segment].

3.2 Toppling failures and aspect ratio

Toppling failures (Figure 6) can occur when a discontinuity or group of discontinuities dip or plunge into the face (Hudson & Harrison 2000). Direct toppling can occur if the centre of gravity of the feature is outside the lower apex of the block and requires a basal plane to serve as either the release plane or a sliding plane. Flexural toppling requires conditions for inter-layer slip to occur and is generally restricted to pervasive fabrics. Direct toppling failures are primarily managed through reduction of bench face angles to <75°, while flexural toppling may require management by reducing inter-ramp angles. The geometric constraints for each toppling failure type differ, and as such the probability of occurrence calculations also differ. The assumption of the presence of a basal plane is still consistent with the initial paper. The results of the toppling assessment are used to identify domains that may require management or prevention of failures through reduction in the bench face or inter-ramp angles.

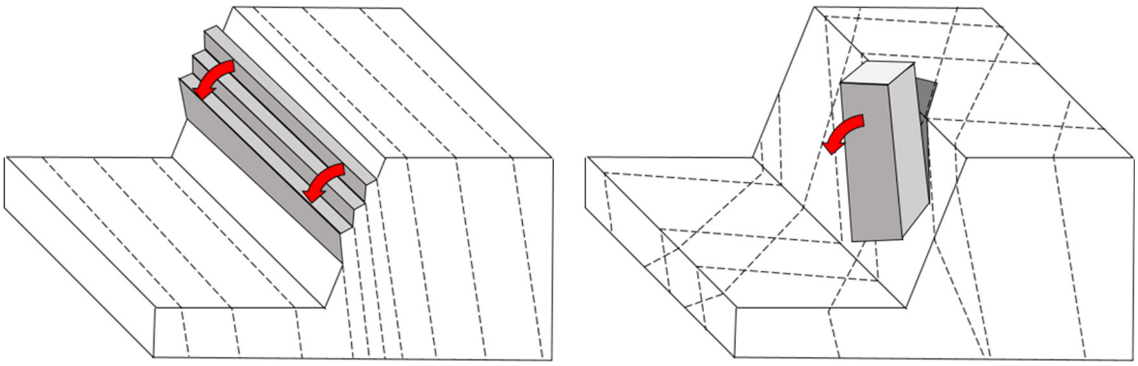

(a) (b)

Figure 6 Flexural (a) and direct (b) toppling failures (after Hudson & Harrison 2000)

3.2.1 Defining aspect ratio

The only significant alteration from the Venter & Hamman (2022) paper are the considerations for block aspect ratio. This calculation assesses the likelihood of forming blocks that are sufficiently tall and slender to form toppling failures. A toppling type failure can only occur if the centre of gravity lies outside of the block (Figure 7). The relationship between the centre of gravity of the block and the dip or plunge of contributing features can be calculated by comparing the ratio of the base (B) to the height (H) of the blocks. Where a block is formed from 2 planes, the intersection line of these planes defines the plunge of the block.

The dimensions of the block, assuming a basal plane is always present, can therefore be described as a function of the spacing and persistence of the contributing discontinuities. Equilibrium occurs when the B/H is equivalent to the tan(dip or plunge) of the block.

Two scenarios can occur depending on the spacing and persistence estimates: the dip or plunge of the feature is less than 45° and greater than 45°. For scenarios where the plunge is greater than 45°, the base length will be equivalent to the spacing, and the height of the block will be described by the persistence.

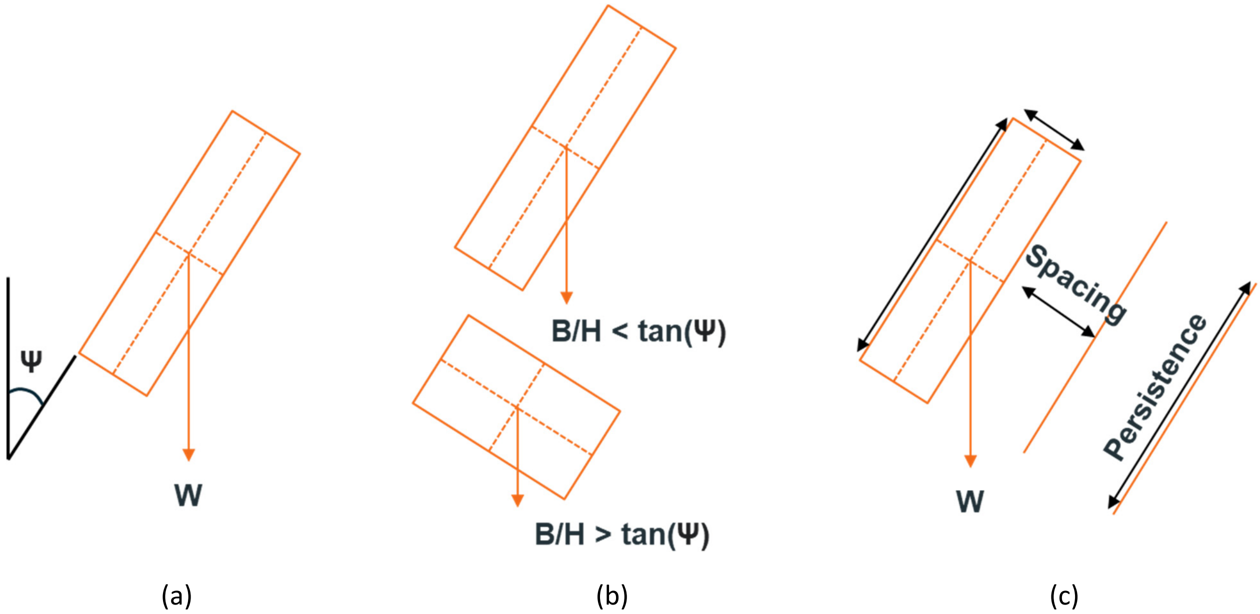

Figure 7 (a) The assumptions for a toppling type failure to occur include a sufficiently shallow dip/plunge (phi) that the centre of gravity is outside of the block; (b) In order for this to occur, the base/height ratio must be smaller than the tan of the plunge line; (c) The block geometry can be described as a function of the spacing and persistence of the contributing joints

3.2.2 Probability that aspect ratio permits toppling (A1)

The aspect ratio of the block is a function of the joint spacing and joint persistence. In order for toppling to occur, the tan(dip or plunge) must be > base/height ratio. For steeper dipping or plunging features (> 45°), the base measurement is the spacing and the height is the persistence. For shallow dipping or plunging features (<45°), the base measurement is the persistence, and the height is the spacing. The persistence and spacing are exponentially distributed and the dip/plunge are normally distributed. For simplicity this assumes that the basal plane is perpendicular to the dip/plunge of the block. Three sub-equations are calculated to determine the probability of having an unfavourable aspect ratio (Equation 4). Considering that a block is defined by the dip of the discontinuity or plunge of the intersection line of 2 discontinuities and the spacing and persistence of the discontinuities, the Equation can be developed by assessing the probability of:

- the base length (nominally the spacing of the discontinuity) being sufficiently narrow enough that slender blocks can be generated
- the height of the block (nominally the persistence of the discontinuity) being sufficiently tall enough that the centre of gravity lies outside of the block footprint
- the dip of the discontinuity or plunge of the block is sufficient to develop a toppling failure.

$$P[Likelihood\ of\ Unfavourable\ Aspect\ Ratio] = \mathrm{A1} = T1 \times T2 \times T3 \quad (4)$$

where:

T1 = P[max base length < tan(dip or plunge) × height]

T2 = P[minimum height > (base length)/tan(dip or plunge)]

T3 = P[tan (dip or plunge) > B/H].

An example of the difference that the inclusion of the aspect ratio check is provided in Figure 8, showing that for the particular project being assessed the aspect ratio consideration removed half of the features from consideration.

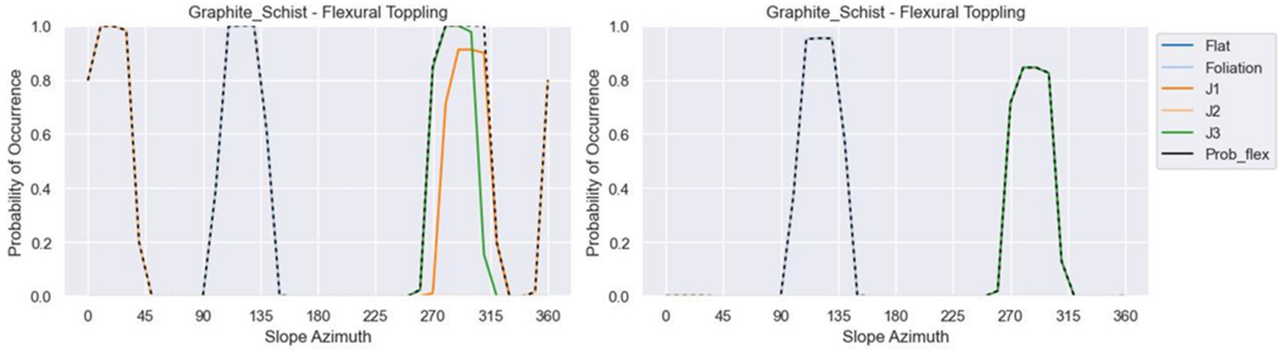

(a) (b)

Figure 8 Example showing the calculations for flexural toppling using (a) the original calculations and (b) the significant reduction in affected sets using the aspect ratio consideration

3.3 Flexural toppling

Flexural toppling considers single plane failures. The potential for flexural toppling is driven primarily by the concept of inter-layer slip. As stresses redistribute normal to the face, the joint dip must be within a critical range to permit flexural toppling to occur. Flexural toppling assessments are generally overly conservative and should instead focus on azimuths affected by persistent fabrics such as foliation or bedding. The probability of occurrence for flexural toppling can occur as a function of the following aspects. Users are advised to filter out joint sets not belonging to fabric as the calculation for flexural toppling.

3.3.1 Probability of occurring within +/− 20° of slope azimuth (F1)

The plane must dip into the slope, within 20° of the slope azimuth. This is a function of the normally distributed range of the discontinuity dip direction.

3.3.2 Probability that dip > 90° − bench face angle + friction angle (F2)

The normally distributed dip of the feature must be greater than the 90° − bench face angle + friction angle for inter-layer slip to occur.

3.3.3 Probability of occurrence for flexural toppling

The probability of occurrence for flexural toppling can be assessed by calculating the probability of achieving each of the geometric constraints shown in Equation 5.

$$P[Flexural\ Toppling] = F1 \times F2 \times A1 \quad (5)$$

where:

F1 = P[ABS(slope azimuth + 180° − discontinuity dip direction) < 20°]

F2 = P[discontinuity dip > 90° − slope angle + friction angle]

A1 = P[likelihood of unfavourable aspect ratio].

3.4 Direct toppling

Direct toppling is assessed considering blocks formed by 2 discontinuity sets. Basal planes are always assumed to be present and favourable for toppling to occur. The probability of occurrence for direct toppling can occur as a function of the following aspects.

3.4.1 Probability of occurring within +/− 20° of slope azimuth (D1)

The intersection line formed by the coincidence of the 2 discontinuities must plunge into the slope, within 20° of the slope azimuth. This is a function of the normally distributed range of the discontinuities.

3.4.2 Probability that dip/plunge < bench face angle (D2)

The normally distributed dip or plunge of the feature must be less than the bench face angle for the failure to occur.

3.4.3 Probability of occurrence for direct toppling

The probability of occurrence for direct toppling can be assessed by calculating the probability of achieving each of the geometric constraints shown in Equation 6.

$$P[Direct\ Toppling] = D1\ \times\ D2\ \times\ D3 \tag{6}$$

where:

D1 = P[ABS(slope azimuth + 180°8722 − trend) < 20°]

D2 = P[plunge < slope angle]

A1 = P[likelihood of unfavourable aspect ratio].

4 Conclusion

The simplified kinematic assessment applied onto pit shells has been invaluable for communicating structurally controlled stability risks for mine design and operations. The ongoing refinements and additions to the calculations presented in this paper have improved the reliability of the results, while adding sufficient flexibility to account for variability in pit shell design options and geological uncertainties. However, the issue of reliably interpolation joint sets for kinematic analysis remains a challenge and deserves further research attention to improve upon this, and other analysis methods.

Acknowledgement

The authors acknowledge both SRK Consulting and AngloGold Ashanti for supporting this cooperative paper. The numerous engineers who provided discussions, critique and suggestions to the original papers, and applied projects, also deserve mention, as it is only through field testing, that real continuous improvement can take place.

References

Basson, F 2025, *GEM4D*, version 1.8.7.1, computer software, BasRock, https://www.basrock.net
Goodman, R 1980, *Introduction to Rock Mechanics*, Wiley, Toronto, pp 254–287.
Goodman, RE & Shi, G 1985, *Block Theory and its Application to Rock Engineering*, Prentice Hall Inc, Englewood Cliff.
Hoek, E & Bray, JW 1981, *Rock Slope Engineering*, revised 3rd edition, The Institution of Mining and Metallurgy, London.
Hudson, JA & Harrison, JP 2000, *Engineering Rock Mechanics: an Introduction to the Principles*, Elsevier, Amsterdam.
Seequent Limited, 2025, *Leapfrog Geo*, version 2025.1, computer software, https://www.seequent.com/products-solutions/leapfrog-geo/
Swan, G & Sepulveda, RS 2001, 'Slope stability at Collahuasi', in WA Hustrulid, in MK McCarter & DJA Van Zyl (eds), *Slope Stability in Surface Mining*, Society for Mining, Metallurgy, and Exploration, Inc, Englewood, pp. 163–170.
Venter, J & Hamman, ECF 2022, 'Kinematic analysis of pit shells', *Proceedings of Slope Stability 2022*, Tucson.
Venter, J, du Plooy, K & Hamman, E 2018, 'Kinematic evalution of pit shell designs using a geotechnical block model', *Proceedings of Slope Stability 2018*, Consejo Superior de Colegios de Ingenieros de Minas & Colegio Oficial de Ingenieros de Minas del Sur, Seville.
Wyllie, D & Mah, C 2004, *Rock Slope Engineering in Civil and Mining*, CRC Press, London.